

# TRANSVERSE CHARGE AND MAGNETIZATION DENSITIES IN THE NUCLEON'S CHIRAL PERIPHERY\*

C. GRANADOS<sup>†</sup> C. WEISS

*Theory Center, Jefferson Lab, Newport News, VA 23606, USA*

In the light-front description of nucleon structure the electromagnetic form factors are expressed in terms of frame-independent transverse densities of charge and magnetization. Recent work has studied the transverse densities at peripheral distances  $b = O(M_\pi^{-1})$ , where they are governed by universal chiral dynamics and can be computed in a model-independent manner. Of particular interest is the comparison of the peripheral charge and magnetization densities. We summarize (a) their interpretation as spin-independent and -dependent current matrix elements; (b) the leading-order chiral effective field theory results; (c) their mechanical interpretation in the light-front formulation; (d) the large- $N_c$  limit of QCD and the role of  $\Delta$  intermediate states; (e) the connection with generalized parton distributions and peripheral high-energy scattering processes.

*Keywords:* Generalized parton distributions, transverse charge and magnetization densities, chiral effective field theory, light-front quantization

PACS numbers: 11.15.Pg, 11.55.Fv, 12.39.Fe, 13.40.Gp, 13.60.Hb, 14.20.Dh  
Report number: JLAB-THY-13-1807

## 1. Transverse charge and magnetization densities

In the light-front description of relativistic systems the transition matrix elements of current operators are expressed in terms of transverse densities.<sup>1,2</sup> They are defined as two-dimensional Fourier transforms of the invariant form factors and describe the distribution of charge and current in the system in transverse space. They are frame-independent (boost-invariant) and represent true densities in the light-front wave functions of composite systems, and thus provide an objective notion of the spatial structure of relativistic systems. Transverse densities have become an essential tool in the study of hadron structure, both in QCD and in approaches based on effective degrees of freedom; see Ref. [3] for a review.

In the context of QCD, the transverse densities correspond to a projection (integral over the light-cone momentum fraction  $x$ ) of the impact parameter-dependent parton densities,<sup>4</sup> which are the transverse spatial representation of the generalized parton distributions (GPDs). The transverse densities in the nucleon thus provide

\*Proceedings of QCD Evolution Workshop, Jefferson Lab, May 6–10, 2013, <http://www.jlab.org/conferences/qcd2013/>

<sup>†</sup>Now at Department of Physics and Astronomy, Nuclear Physics, Uppsala University, Box 516, 75120 Uppsala, Sweden

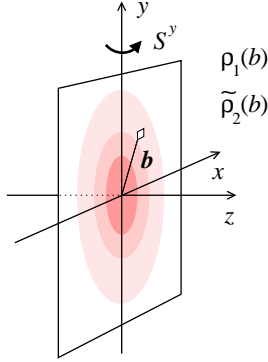


Fig. 1. Interpretation of the transverse densities associated with the electromagnetic current, Eq. (2).  $\rho_1(b)$  describes the spin-independent part of the  $J^+$  current in a nucleon state with its transverse center-of-momentum localized at the origin;  $\tilde{\rho}_2(b)$ , Eq. (3), describes the spin-dependent part in a nucleon polarized in the positive  $y$ -direction.

indirect information on the distribution of partons in transverse space, and open an interesting connection between low-energy elastic  $eN/\nu N$  scattering and high-energy inelastic processes resolving the nucleon's quark/gluon content. Considerable efforts have been devoted to constructing empirical charge and magnetization densities in the nucleon from the available elastic form factor data.<sup>3</sup>

The nucleon electromagnetic current matrix element is described by the transverse charge and magnetization densities, defined as the Fourier transforms of the Dirac and Pauli form factors,  $F_1(t)$  and  $F_2(t)$ , in a frame where the momentum transfer to the nucleon is in the transverse direction,

$$\rho_{1,2}(b) = \int \frac{d^2 \Delta_T}{(2\pi)^2} e^{-i\Delta_T b} F_{1,2}(t = -\Delta_T^2). \quad (1)$$

Their integral over transverse space gives the total charge and anomalous magnetic moment. The interpretation of  $\rho_{1,2}(b)$  as spatial densities has been discussed extensively in the literature.<sup>2,3,4</sup> In a state where the nucleon is localized in transverse space at the origin, and polarized in the  $y$ -direction, the matrix element of the “plus” component of the current,  $J^+ \equiv J^0 + J^z$ , at  $x^\pm = 0$  and  $\mathbf{x}_T = \mathbf{b}$ , is given by

$$\langle J^+(\mathbf{b}) \rangle = (\dots) [\rho_1(b) + (2S^y) \cos \phi \tilde{\rho}_2(b)], \quad (2)$$

$$\tilde{\rho}_2(b) \equiv \frac{\partial}{\partial b} \left[ \frac{\rho_2(b)}{2M_N} \right], \quad (3)$$

where (...) hides a trivial factor reflecting the normalization of states,  $\cos \phi \equiv b^x/b$  is the cosine of the azimuthal angle, and  $S^y = \pm 1/2$  the spin projection in the  $y$ -direction in the nucleon rest frame. The function  $\rho_1(b)$  describes the spin-independent part of the current, the function  $\tilde{\rho}_2(b)$  the spin-dependent part in a transversely polarized nucleon (see Fig. 1). The latter changes sign between positive and negative values of  $b^x$  (“right” and “left,” when looking at the nucleon in the  $z$ -direction from  $+\infty$ ), as would be expected for a convection current due to rotational motion around the  $y$ -axis. A basic question of nucleon structure is how the ratio  $\tilde{\rho}_2(b)/\rho_1(b)$  behaves as a function of the transverse position  $b$ , particularly in regions

where a simple dynamical interpretation is possible. Intuition from non-relativistic systems suggests that  $\rho_1$  counts the number of constituents per transverse area, while  $\tilde{\rho}_2(b)$  measures the current, so that the ratio should reflect the velocity of the internal motion of the constituents. The concept of transverse densities allows one to pose the question rigorously also for relativistic systems.

At large distances the behavior of strong interactions is dominated by the spontaneous breaking of chiral symmetry. The associated quasi-massless excitations (Goldstone bosons), the pions, couple weakly to hadronic matter and mediate low-energy interactions over distances of the order  $M_\pi^{-1}$ , much larger than the bulk hadronic size. In current matrix elements they induce characteristic contributions in which the current couples to the hadron by exchange of “soft” pions with momenta  $k_\pi \sim M_\pi$ . In the transverse densities they give rise to distinctive long-range components at  $b = O(M_\pi^{-1})$ , which can be calculated model-independently and represent fundamental chiral properties of the structure. They are analogous to the well-known “Yukawa tails” of non-relativistic physics but have a precise relativistic meaning. Recent theoretical work<sup>5,6</sup> has studied the chiral component of the transverse charge and magnetization densities using methods of chiral effective field theory (EFT). It observed an interesting inequality<sup>5</sup> between the leading-order spin-dependent and independent peripheral densities, and suggested a simple explanation in a mechanical picture based on the first-quantized light-front formulation of chiral EFT. It also investigated the scaling behavior of the transverse densities in the large- $N_c$  limit of QCD and showed that inclusion of  $\Delta$  intermediate states guarantees the proper scaling of the pionic component. These findings provide model-independent constraints on the peripheral transverse densities at large  $b$  and enable an intuitive understanding of chiral nucleon structure. Here we summarize the main points, focusing on the comparison of  $\tilde{\rho}_2$  and  $\rho_1$ ; for the conceptual and practical aspects of chiral EFT in peripheral transverse densities we refer to the original article.<sup>5</sup>

## 2. Peripheral densities from chiral EFT

The large-distance behavior of transverse densities can conveniently be studied in a dispersive representation,<sup>6</sup> in which they are expressed as integrals over the imaginary parts (or spectral functions) of the invariant form factors on the principal cut in the timelike region,

$$\rho_{1,2}(b) = \int_{4M_\pi^2}^{\infty} \frac{dt}{2\pi} K_0(\sqrt{tb}) \frac{\text{Im} F_{1,2}(t + i0)}{\pi}. \quad (4)$$

In this formulation the densities as  $b = O(M_\pi^{-1})$  are the “image” of the spectral functions on the two-pion cut at  $t = 4M_\pi^2 = O(M_\pi^2)$ , which can systematically be computed in chiral EFT and have been studied extensively in the literature.<sup>7,8,9,10</sup> In the leading-order (LO) approximation of relativistic chiral EFT,<sup>11</sup> the isovector spectral functions [ $V \equiv (p - n)/2$ ] are given by the chiral processes of Fig. 2a, where

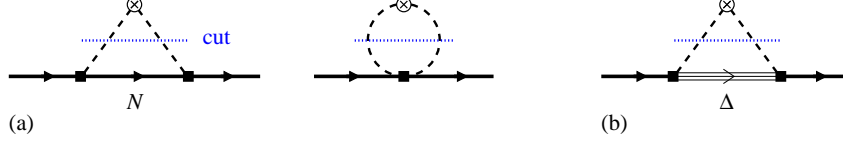


Fig. 2. (a) LO chiral EFT processes contributing to the two-pion cut of the isovector nucleon form factors and the peripheral charge and magnetization densities. (b) Intermediate  $\Delta$  contribution.

the current couples to the nucleon by two-pion exchange, and the pion-nucleon vertices are those of the LO chiral Lagrangian. Evaluation of the chiral component of the densities is straightforward, and analytic approximations can be derived. The general form of the peripheral densities at  $b = O(M_\pi^{-1})$  is

$$\rho_1^V(b), \tilde{\rho}_2^V(b) = e^{-2M_\pi b} \times \text{functions}(M_\pi, M_N; b), \quad (5)$$

where the exponential behavior is dictated by the minimum mass of the exchanged two-pion system in the  $t$ -channel and the pre-exponential functions reflect the complexity of its coupling to the nucleon. In leading order of  $M_\pi/M_N$  (heavy-baryon expansion) one finds that

$$\tilde{\rho}_2^V(b)/\rho_1^V(b) = O[(M_\pi/M_N)^0] \equiv O(1) \quad [b = O(M_\pi^{-1})]. \quad (6)$$

The spin-independent and -dependent parts of the isovector current matrix element Eq. (3) are of the same order in the chiral region. This shows that it is natural to work with  $\tilde{\rho}_2$  instead of  $\rho_2$ ; for the original  $\rho_2$  the corresponding ratio is  $\rho_2/\rho_1 = O(M_N/M_\pi)$ . The numerical results for the LO densities in the chiral region (see Fig. 3) show that in this approximation the spin-dependent density is bounded by the spin-independent one,

$$|\tilde{\rho}_2^V(b)| < \rho_1^V(b). \quad (7)$$

The inequality is practically saturated at distances  $b \sim \text{few } M_\pi^{-1}$ ; at larger distances the spin-dependent density becomes systematically smaller than the spin-independent one. We emphasize that Eq. (7) is specific to the LO chiral EFT result and can be modified by higher-order corrections;<sup>9,10</sup> it also ceases to be valid when  $\Delta$  intermediate states are included as required by the large- $N_c$  limit of QCD (see below). Still, it is interesting to inquire about the dynamical origin of this surprising observation.

### 3. Mechanical picture in light-front quantization

A more intuitive understanding of the structure of the LO chiral component, can be obtained in a first-quantized mechanical picture, where one follows the evolution of chiral EFT processes in light-front time  $x^+$ .<sup>12</sup> In this formulation the peripheral densities arise from processes in which the initial nucleon “fluctuates” into a large-size pion-nucleon ( $\pi N$ ) system through the perturbative chiral EFT interaction.

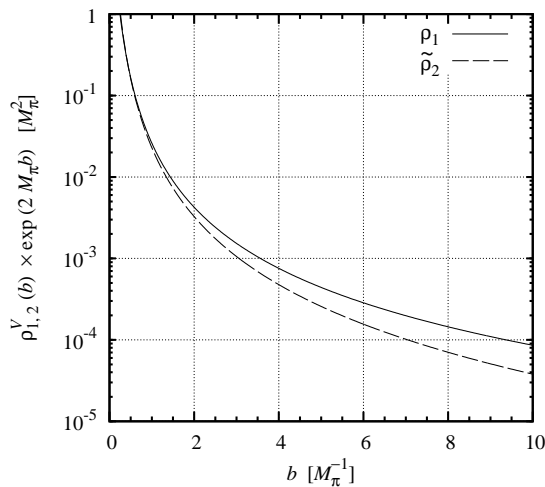


Fig. 3. LO chiral component of the nucleon's isovector transverse spin-independent density  $\rho_1^V(b)$  (solid line) and spin-dependent density  $\tilde{\rho}_2^V(b)$  (dashed line).<sup>5</sup> The plot shows the densities with the exponential factor  $\exp(-2M_\pi b)$  extracted [the functions plotted correspond to the pre-exponential factor in Eq. (5)]. The distance  $b$  is given in units of  $M_\pi^{-1}$ , the densities in units of  $M_\pi^2$ .

The process is described by light-front wave functions  $\psi_{0,1}(y, r_T)$  (see Fig. 4a), which depend on the pion light-cone momentum fraction  $y = O(M_\pi/M_N)$ , the transverse spatial separation  $r_T = O(M_\pi^{-1})$  of the final  $\pi N$  system, and the light-front helicities of the initial and final nucleon (helicity-conserving,  $\psi_0$ ; helicity-flip,  $\psi_1$ ; the dependence on the transverse angle  $\phi$  is dictated by angular momentum conservation and can be separated<sup>12</sup>). The peripheral isovector densities can then be expressed as overlap integrals of the light-front wave functions (see Fig. 4b),

$$\left. \begin{aligned} \rho_1^V(b) \\ \tilde{\rho}_2^V(b) \end{aligned} \right\} = \int \frac{dy}{2\pi y \bar{y}^3} \left\{ \begin{aligned} & [|\psi_0(y, r_T)|^2 + |\psi_1(y, r_T)|^2]_{r_T=b/\bar{y}} + \text{instant.}, \\ & [\psi_0^\dagger(y, r_T) \psi_1(y, r_T) + \psi_1^\dagger(y, r_T) \psi_0(y, r_T)]_{r_T=b/\bar{y}}, \end{aligned} \right. \quad (8)$$

where  $\bar{y} \equiv 1 - y$ . The inequality Eq. (7) follows directly from the quadratic forms in the integrand of Eq. (8). It holds up to an instantaneous term  $\propto \delta(y)$  in  $\rho_1$ , which represents the cumulative effect of high-mass intermediate states not resolved in chiral EFT; this term is proportional to  $(1 - g_A^2)$  and numerically small.<sup>5</sup> Likewise, Eq. (6) can be inferred from the parametric order of the wave functions.<sup>12</sup> These results show that the light-front formulation of chiral EFT provides genuine new insight into chiral nucleon structure and demonstrates the usefulness of the transverse densities as quantities with a direct interpretation in terms of light-front wave functions.

Alternatively, one may characterize the nucleon polarization in Eq. (8) by its transverse spin in the rest frame. This leads to an even simpler mechanical picture:<sup>5</sup> the nucleon with transverse spin projection  $S^y = +1/2$  fluctuates into a  $\pi N$  system, where the intermediate  $N$  has spin projection  $-1/2$  and the  $\pi$  orbits with  $L^y = +1$  around the  $y$  axis. The ratio of spin-dependent and -independent peripheral densities is of the order of the pion velocity,  $v = k_\pi/M_\pi = O(1)$ , which naturally explains Eq. (6). This picture is maximally close to the non-relativistic intuition

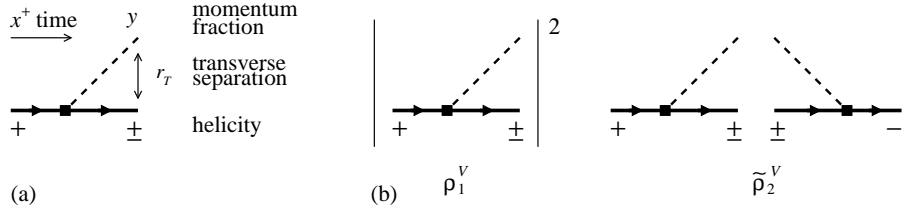


Fig. 4. (a) Light-front wave function of the  $\pi N$  system in chiral EFT. (b) Wave function overlap representation of the transverse densities  $\rho_1$  (helicity-conserving) and  $\tilde{\rho}_2$  (helicity-flip).

and takes advantage of the fact that the light-front description is boost-invariant and can be implemented in any frame, including the rest frame. Details will be provided elsewhere.<sup>12</sup>

#### 4. $\Delta$ intermediate states and large- $N_c$ limit

Other interesting information on the peripheral transverse densities comes from the large- $N_c$  limit of QCD.<sup>5</sup> The  $N_c$ -scaling of integral nucleon observables (charges, magnetic moments) has been studied extensively in the literature<sup>13,14</sup> and provides useful constraints for dynamical models and phenomenological analysis. The same techniques can be applied to study the transverse densities at non-exceptional distances  $b = O(N_c^0)$ , which includes the chiral region  $b = O(M_\pi^{-1})$ , as  $M_\pi = O(N_c^0)$ . One finds that the isovector densities in large- $N_c$  QCD scale as

$$\rho_1^V(b) = O(N_c^0), \quad \tilde{\rho}_2^V(b) = O(N_c) \quad [b = O(N_c^0)]. \quad (9)$$

The spin-dependent density is parametrically larger than the spin-independent one, reflecting a general property of the spin-flavor wave function of the large- $N_c$  nucleon. It implies that the inequality Eq. (7), observed in the LO chiral EFT result, is not compatible with the large- $N_c$  limit of QCD. Indeed, one finds that the spin-independent density obtained in LO chiral EFT exhibits a “wrong”  $N_c$ -scaling as  $\rho_1^V(b) = O(N_c)$ .

This is not surprising, as it is well-known that in the large- $N_c$  limit the  $\Delta$  isobar becomes degenerate with the  $N$  and needs to be included as an intermediate state in the two-pion spectral function on the same footing (see Fig. 2b).<sup>15,16</sup> Using a phenomenological  $\pi N \Delta$  coupling it was shown explicitly<sup>5</sup> that in the large- $N_c$  limit the intermediate  $\Delta$  contribution *cancels* the  $N$  one in  $\rho_1(b)$  to leading order in  $1/N_c$ , while it *adds* to the  $N$  in  $\tilde{\rho}_2^V(b)$ . Inclusion of the  $\Delta$  thus “restores” the proper  $N_c$ -scaling of the two-pion component of the peripheral transverse charge density, and one obtains

$$\rho_1^V(b)_N + \rho_1^V(b)_\Delta = O(N_c^0), \quad (10)$$

$$\tilde{\rho}_2^V(b)_N + \tilde{\rho}_2^V(b)_\Delta = O(N_c) \quad [b = O(N_c^0)], \quad (11)$$

in accordance with Eq. (9). The  $\Delta$  thus plays an essential qualitative role in the large- $N_c$  limit. Numerically, with the empirical values of the  $N$ - $\Delta$  mass splitting

and  $\pi N\Delta$  coupling, the  $\Delta$  contribution to the peripheral densities is  $\lesssim 20\%$  of the  $N$  at  $b > 2M_\pi^{-1}$  in both cases, so that the chiral EFT result with  $N$  only still provides a valid approximation.

The fact that the spin-dependent component of the isovector transverse density is parametrically leading in the large- $N_c$  limit suggests that it may also be numerically larger than the spin-independent one. This question could be addressed in dynamical models based on the large- $N_c$  limit, which describe the nucleon as a chiral soliton (skyrmion,<sup>17</sup> chiral quark-soliton model<sup>18</sup>). In these models the  $N$  and  $\Delta$  correspond to different rotational states of the classical soliton, and the contribution from  $\Delta$  intermediate states is effectively included in the peripheral densities.<sup>15,16</sup>

## 5. Empirical densities and experimental tests

Chiral dynamics and the large- $N_c$  limit of QCD provide model-independent theoretical insight into the structure of the nucleon's peripheral transverse charge and magnetization (or spin-independent and dependent) densities. Important practical questions are how one should construct empirical densities incorporating these constraints, and whether one could probe the chiral component of the transverse densities directly in scattering experiments.

A numerical study of the nucleon's transverse densities<sup>19</sup> using the dispersion integral Eq. (4) shows that the chiral two-pion component becomes numerically dominant only at large distances  $b \gtrsim 2$  fm. At smaller distances the densities (isovector and isoscalar) are overwhelmingly generated by the vector meson resonances ( $\rho, \omega$ ) in the spectral function. Realistic transverse densities are therefore best constructed by evaluating the dispersion integral Eq. (4) with empirical spectral functions, which include the chiral two-pion component near threshold (as described by chiral EFT), the vector meson resonances, and a continuum of higher-mass states determined by fits to the spacelike form factor data.<sup>20,21</sup> This formulation implements the proper analytic structure of the form factor near threshold, which guarantees the correct large-distance asymptotic behavior of the densities.

The chiral component at large  $b$  makes a distinctive contribution to the  $b^{2n}$ -weighted moments ( $n = 1, 2, \dots$ ) of the transverse densities, which are related to the  $n$ 'th derivatives of the elastic form factors at  $t = 0$ .<sup>5</sup> A preliminary assessment<sup>6</sup> found that the chiral component of the isovector density contributes only  $\sim 20\%$  to the  $b^2$ -weighted moment, but  $O(1)$  to the  $b^4$ -weighted and higher moments. This suggests that the chiral component causes “unnatural” behavior of the second and higher derivatives of the form factors at  $t = 0$ , which might be observable in combined fits to low- $|t|$  elastic scattering data and atomic physics measurements of the proton charge radius.<sup>22,23</sup>

The chiral component of transverse nucleon structure can also be probed in peripheral high-energy scattering processes, e.g. deep-inelastic or exclusive processes which resolve the peripheral quark/gluon structure with a momentum trans-

fer  $Q^2 \gg 1 \text{ GeV}^2$ . An important point is that the chiral light-front wave functions of the peripheral  $\pi N$  system are universal and determine also the nucleon's peripheral quark/gluon densities,<sup>24</sup> or the amplitudes for peripheral exclusive processes with pion production, when supplemented with the appropriate information about pion structure. One promising candidate is hard exclusive electroproduction (of vector mesons, photons etc.) on a peripheral pion that is observed in the final state together with the remnant nucleon;<sup>25</sup> such types of processes could be studied with a future Electron-Ion Collider (EIC).<sup>26,27</sup> The advantage of the light-front formulation of nucleon structure is precisely that it connects low-energy elastic form factors with observables in peripheral high-energy scattering processes in a well-defined manner, greatly enlarging the number of available probes.

**Notice:** Authored by Jefferson Science Associates, LLC under U.S. DOE Contract No. DE-AC05-06OR23177. The U.S. Government retains a non-exclusive, paid-up, irrevocable, world-wide license to publish or reproduce this manuscript for U.S. Government purposes.

## References

1. D. E. Soper, Phys. Rev. D **15**, 1141 (1977).
2. G. A. Miller, Phys. Rev. Lett. **99**, 112001 (2007).
3. G. A. Miller, Ann. Rev. Nucl. Part. Sci. **60**, 1 (2010).
4. M. Burkardt, Phys. Rev. D **62**, 071503 (2000) [Erratum-ibid. D **66**, 119903 (2002)]; Int. J. Mod. Phys. A **18**, 173 (2003).
5. C. Granados and C. Weiss, arXiv:1308.1634 [hep-ph].
6. M. Strikman and C. Weiss, Phys. Rev. C **82**, 042201 (2010).
7. J. Gasser, M. E. Sainio and A. Svarc, Nucl. Phys. B **307**, 779 (1988).
8. V. Bernard, N. Kaiser and U.-G. Meissner, Nucl. Phys. A **611**, 429 (1996).
9. B. Kubis and U.-G. Meissner, Nucl. Phys. A **679**, 698 (2001).
10. N. Kaiser, Phys. Rev. C **68**, 025202 (2003).
11. T. Becher and H. Leutwyler, Eur. Phys. J. C **9**, 643 (1999).
12. C. Granados and C. Weiss, in preparation
13. E. Witten, Nucl. Phys. B **160**, 57 (1979).
14. R. F. Dashen, E. E. Jenkins and A. V. Manohar, Phys. Rev. D **49**, 4713 (1994) [Erratum-ibid. D **51**, 2489 (1995)]; Phys. Rev. D **51**, 3697 (1995).
15. T. D. Cohen and W. Broniowski, Phys. Lett. B **292**, 5 (1992).
16. T. D. Cohen, Rev. Mod. Phys. **68**, 599 (1996).
17. I. Zahed and G. E. Brown, Phys. Rept. **142**, 1 (1986).
18. C. V. Christov *et al.*, Prog. Part. Nucl. Phys. **37**, 91 (1996).
19. G. A. Miller, M. Strikman and C. Weiss, Phys. Rev. C **84**, 045205 (2011).
20. M. A. Belushkin, H.-W. Hammer and U.-G. Meissner, Phys. Rev. C **75**, 035202 (2007).
21. I. T. Lorenz, H.-W. Hammer and U.-G. Meissner, Eur. Phys. J. A **48**, 151 (2012).
22. J. C. Bernauer *et al.* [A1 Collaboration], arXiv:1307.6227 [nucl-ex].
23. A. Gasparian *et al.*, Jefferson Lab 12 GeV Experiment E12-11-106, [http://www.jlab.org/exp\\_prog/proposals/11/PR12-11-106.pdf](http://www.jlab.org/exp_prog/proposals/11/PR12-11-106.pdf)
24. M. Strikman and C. Weiss, Phys. Rev. D **80**, 114029 (2009).
25. M. Strikman and C. Weiss, Phys. Rev. D **69**, 054012 (2004).
26. A. Accardi, V. Guzey, A. Prokudin and C. Weiss, Eur. Phys. J. A **48**, 92 (2012).
27. A. Accardi *et al.*, arXiv:1212.1701 [nucl-ex].